

A Modified Construction Method of Blended Rolled Edge and Its Application

Yongquan Jiang^{1, 2, *}, Hongcheng Yin^{1, 2}, Chongjiang Mo¹, and Dewang Kong¹

Abstract—It is of great practical value to study the blended rolled edge of reflector used in Compact Antenna Test Range (CATR). Taking a rectangular aperture reflector as the benchmark, a reflector with ideal blended rolled edge is obtained by means of parameter iterative optimization after accurately establishing the position relationship between the local and global coordinates where the blended rolled edge is located, precisely deriving the geometric equation of the main reflector zone and blended rolled edge zone in the local coordinate and optimizing continuity condition of curvature radius. On the basis, a blended rolled edge reflector with minimum operating frequency of 0.8 GHz and quiet zone size of 2 m is designed. The simulation results show that the performance of the reflector with blended rolled edge obtained by the proposed method is better than that obtained by the traditional construction method, and the designed reflector has excellent performance. The work in this paper provides a theoretical support for the optimal design and engineering application of the blended rolled edge reflector.

1. INTRODUCTION

Compact Antenna Test Range (CATR) is a general term for a kind of electromagnetic measuring equipment, who can convert spherical wave emitted by the feed into plane wave through a high-precision reflector at a short distance. This kind of equipment is used to imitate far-field test conditions in a specific area called quiet zone, whose shape seems like inverted cylinder, as shown in Figure 1. According to the geometric form and quantity, the reflector can be classified as single paraboloid, single parabolic cylinder, double parabolic cylinder, double Gregorian reflectors, double Cassegrain reflectors, etc., among which single offset paraboloid is the most commonly and widely used.

In consideration of reducing the influence of the diffraction field caused by reflector edge on the field distribution in quiet zone, the reflector edge needs to be shaped. Once the reflector used in CATR was invented in the 1970s [1], the form of follow-up sharp teeth has been adopted in the design of reflector edge, which is still used today. Although the sharp teeth has derived various shapes during this period [2], its low-frequency performance still cannot fully meet the actual use requirements. From 1984 to 1997 [3–16], Professor Burnside’s team creatively put forward the concept and construction method of blended rolled edge and proved the advantages of this kind of edge processing method in improving the low-frequency performance of reflector. This method was widely used by researchers in the design of reflector used in CATR afterward, which is suitable for low-frequency testing [17–20]. Recently, when designing the blended rolled edge reflector used in practical engineering, the authors found that the former construction method involves some problems, such as inaccurate selection of local coordinate and approximate treatment of the equation of the main reflector zone in local coordinate, which will affect the aperture shape of the reflector and limit the low-frequency performance of the quiet zone. This reason prompted the authors to reexamine the former method.

Received 24 March 2022, Accepted 26 April 2022, Scheduled 7 May 2022

* Corresponding author: Yongquan Jiang (362790370@qq.com).

¹ Science and Technology on Electromagnetic Scattering Laboratory, Beijing 100854, China. ² School of Information and Communication Engineering, Communication University of China, Beijing 100024, China.

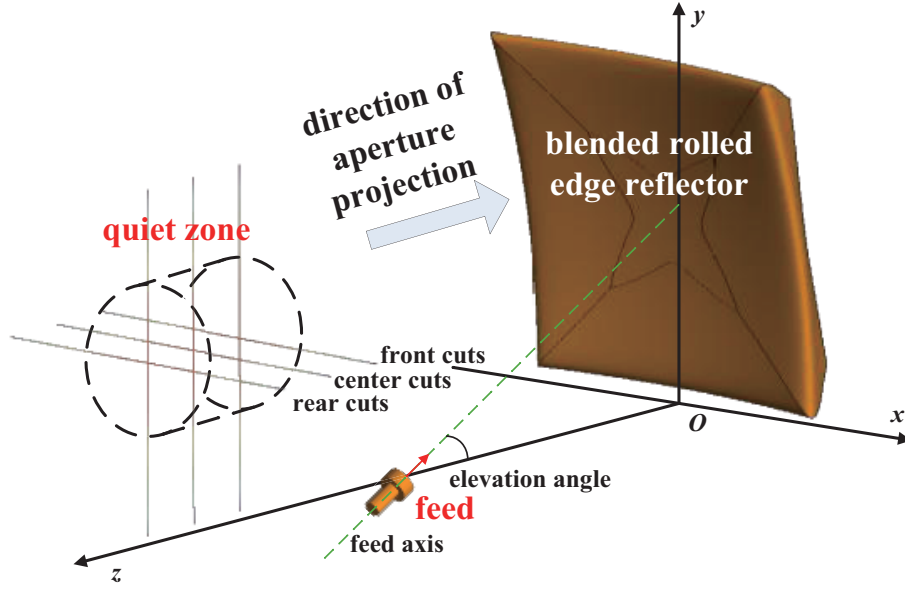


Figure 1. Operating principle of reflector in CATR.

By establishing new local coordinate, accurately solving the equation of the main reflector in the local coordinate and optimizing the continuity condition of curvature radius, this paper proposes a modified construction method of blended rolled edge, so as to obtain the blended rolled edge reflector whose geometric shape and electromagnetic performance fully meet the requirements, and design a reflector with minimum working frequency of 0.8 GHz and quiet zone size of 2 m. Finally, the correctness of this modified method and the superiority of the performance of the designed reflector are verified by the geometric model and simulation results.

2. TRADITIONAL CONSTRUCTION METHOD OF BLENDED ROLLED EDGE

In order to restrict the size and shape of the reflector, the parameters of aperture projection in the xoy plane are usually well designed. The projection parameters of rectangular aperture can be defined as follows [9, 13]: the coordinate of points on aperture outline is (x_{ax}, y_{ax}) ; the coordinate of central point in this aperture is (x_{avg}, y_{avg}) ; the maximum and minimum values of this aperture in the x -axis direction are x_{max} and x_{min} , respectively, and the maximum and minimum values in the y -axis direction are y_{max} and y_{min} , respectively, which satisfy the relationship:

$$x_{avg} = (x_{max} + x_{min})/2 \quad (1)$$

$$y_{avg} = (y_{max} + y_{min})/2 \quad (2)$$

Assuming that the connection point between the main reflector zone and the blended rolled edge is $P_j(x_j, y_j, z_j)$ in 3D coordinate, and the absolute length of blended rolled edge is r_e , the coordinate components of connection point P_j can be expressed as:

$$x_j = x_{ax} - \frac{r_e (x_{ax} - x_{avg})}{\sqrt{(x_{ax} - x_{avg})^2 + (y_{ax} - y_{avg})^2}} \quad (3)$$

$$y_j = y_{ax} - \frac{r_e (y_{ax} - y_{avg})}{\sqrt{(x_{ax} - x_{avg})^2 + (y_{ax} - y_{avg})^2}} \quad (4)$$

$$z_j = \frac{x_j^2 + y_j^2}{4f_c} \quad (5)$$

where f_c represents the focal length of the reflector, and all parameters above are shown in Figure 2.

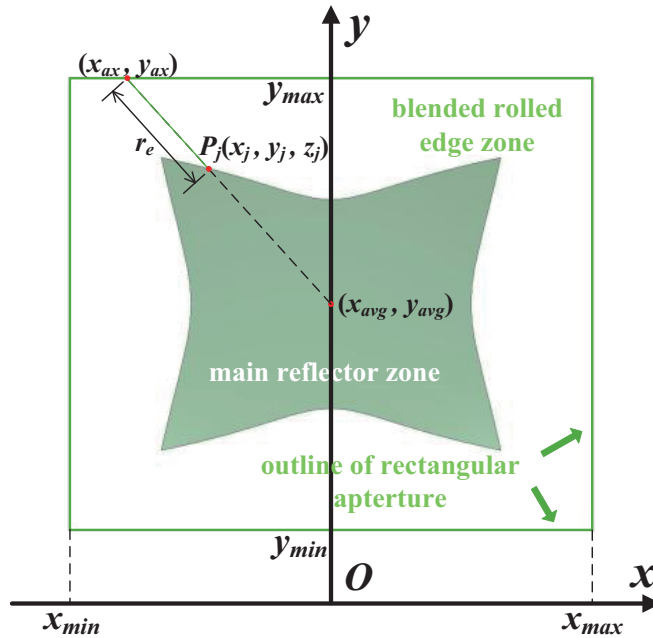


Figure 2. Parameters in rectangular projection.

The blended rolled edge zone in Figure 2 is composed of curved surfaces obtained by sweeping all the blended rolled edge curves on each side. The specific construction of blended rolled edges is shown in Figure 3.

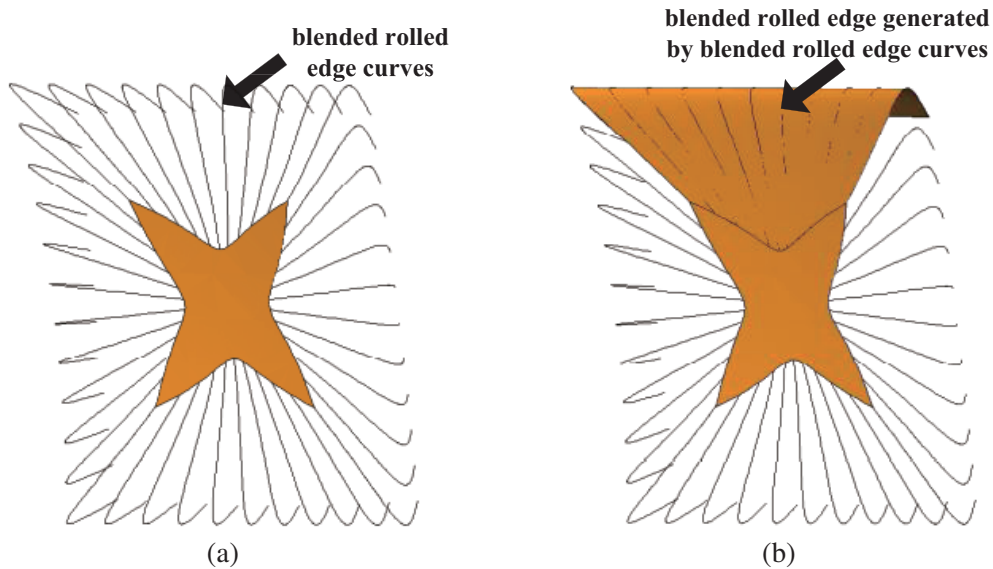


Figure 3. Construction of blended rolled edges. (a) Main reflector and blended rolled edge curves. (b) Main reflector, blended rolled edge curves and blended rolled edge upside.

In order to easily solve the equations corresponding to blended rolled edge curves on each side, it is necessary to establish a local coordinate (x_e, y_e, p) at P_j . In [9] and [13], firstly, the normal direction at P_j is determined as the negative direction of y_e , and then the unit vector along y_e -axis can be expressed as:

$$\hat{y}_e = -\hat{n}_j = y_{p1}\hat{x} + y_{p2}\hat{y} + y_{p3}\hat{z} \tag{6}$$

where \hat{x} , \hat{y} , and \hat{z} represent the unit vector along x -axis, y -axis, and z -axis in global coordinate, respectively, and meet that:

$$y_{p1} = \frac{x_j}{\sqrt{x_j^2 + y_j^2 + 4f_c^2}} \quad (7)$$

$$y_{p2} = \frac{y_j}{\sqrt{x_j^2 + y_j^2 + 4f_c^2}} \quad (8)$$

$$y_{p3} = \frac{-2f_c}{\sqrt{x_j^2 + y_j^2 + 4f_c^2}} \quad (9)$$

Then the direction perpendicular to the projection line of local coordinate is determined as the p -axis, and its unit vector is defined as:

$$\hat{p} = p_1\hat{x} + p_2\hat{y} \quad (10)$$

Since the projection line passes through P_j and the central point of rectangular aperture, p_1 and p_2 can be expressed as:

$$p_1 = -\frac{y_j - y_{\text{avg}}}{\sqrt{(x_j - x_{\text{avg}})^2 + (y_j - y_{\text{avg}})^2}} \quad (11)$$

$$p_2 = \frac{x_j - x_{\text{avg}}}{\sqrt{(x_j - x_{\text{avg}})^2 + (y_j - y_{\text{avg}})^2}} \quad (12)$$

The unit vector of x_e -axis satisfies that:

$$\hat{x}_e = \frac{\hat{y}_e \times \hat{p}}{|\hat{y}_e \times \hat{p}|} = x_{p1}\hat{x} + x_{p2}\hat{y} + x_{p3}\hat{z} \quad (13)$$

where,

$$x_{p1} = -\frac{y_{p3}p_2}{\sqrt{(y_{p3}p_2)^2 + (y_{p3}p_1)^2 + (y_{p1}p_2 - y_{p2}p_1)^2}} \quad (14)$$

$$x_{p2} = \frac{y_{p3}p_1}{\sqrt{(y_{p3}p_2)^2 + (y_{p3}p_1)^2 + (y_{p1}p_2 - y_{p2}p_1)^2}} \quad (15)$$

$$x_{p3} = \frac{y_{p1}p_2 - y_{p2}p_1}{\sqrt{(y_{p3}p_2)^2 + (y_{p3}p_1)^2 + (y_{p1}p_2 - y_{p2}p_1)^2}} \quad (16)$$

The position of this local coordinate in global coordinate is shown in red in Figure 4 at P_j .

The transformation relationship between the local coordinate (x_e, y_e, p) and the global coordinate (x, y, z) at P_j is expressed as:

$$\begin{bmatrix} x_e \\ y_e \end{bmatrix} = \begin{bmatrix} x_{p1} & x_{p2} & x_{p3} \\ y_{p1} & y_{p2} & y_{p3} \end{bmatrix} \begin{bmatrix} x - x_j \\ y - y_j \\ z - z_j \end{bmatrix} \quad (17)$$

$$\begin{bmatrix} x \\ y \\ z \end{bmatrix} = \begin{bmatrix} x_{p1} & y_{p1} \\ x_{p2} & y_{p2} \\ x_{p3} & y_{p3} \end{bmatrix} \begin{bmatrix} x_e \\ y_e \end{bmatrix} + \begin{bmatrix} x_j \\ y_j \\ z_j \end{bmatrix} \quad (18)$$

Then the blended rolled edge needs to be constructed in the local coordinate at P_j . It is assumed that the blended rolled edge is formed by the transition from section part on main reflector to ellipse, that is:

$$f_{\text{blend}}(\gamma) = f_{\text{curve}}(\gamma) [1 - b(\gamma)] + f_{\text{ellipse}}(\gamma) b(\gamma) \quad (19)$$

Among them, γ represents the radian corresponding to the angle of rotation from negative direction of the y_e -axis to its positive direction; $f_{\text{blend}}(\gamma)$ represents the blended rolled edge equation; $f_{\text{curve}}(\gamma)$

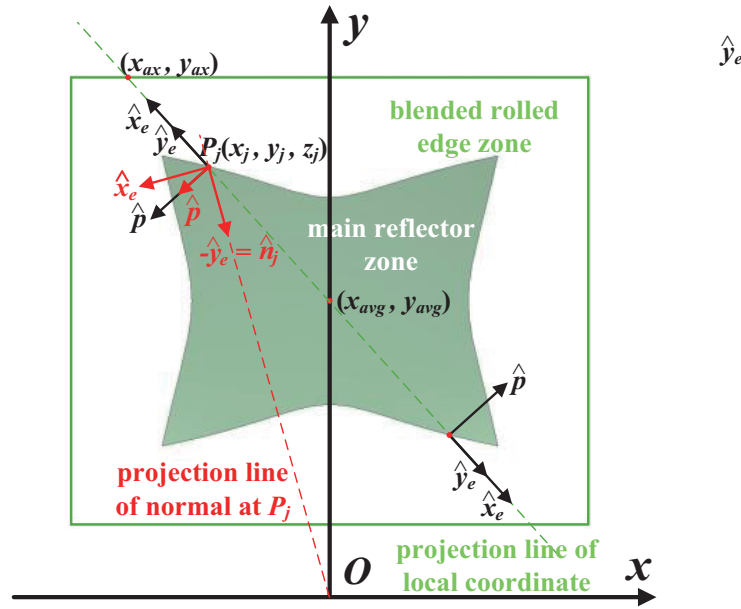


Figure 4. Position relationship between local coordinate and global coordinate.

represents the section equation of the main reflector; $f_{\text{ellipse}}(\gamma)$ represents the elliptic equation; $b(\gamma)$ represents the transition function and satisfies that when $\gamma = 0$, $b(\gamma) = 0$, and when $\gamma = \gamma_m$, $b(\gamma) = 1$; γ_m represents the maximum rotation angle. Considering the highest derivative order as possible, the expression of $b(\gamma)$ is determined as:

$$b(\gamma) = \frac{1}{4} \left(1 - \cos \frac{\pi\gamma}{\gamma_m} \right)^2 \tag{20}$$

Assuming that the length of blended rolled edge curve corresponds to that of extended line on main reflector, and there is a linear relationship between them:

$$f_{\text{curve}}(\gamma) = \frac{x_m}{\gamma_m} \gamma \hat{x}_e \tag{21}$$

In [9] and [13], the section part of main reflector is approximately equivalent to a parabola in local coordinate, and then the concept of equivalent parabola is derived. By randomly selecting two groups of points on the equivalent parabola in local coordinate, the focal length f_c' and the height of connection point y_j' can be solved, and the equation of equivalent parabola in local coordinate is obtained.

The elliptic equation in local coordinate can be expressed as:

$$f_{\text{ellipse}}(\gamma) = a_e \sin \gamma \hat{x}_e + b_e (1 - \cos \gamma) \hat{y}_e \tag{22}$$

where a_e and b_e represent the semi-major and semi-minor axes of the ellipse, respectively.

Then the parametric equation of blended rolled edge in global coordinate can be solved by combining with Equations (18) and (19). The parameters of blended rolled edge in local coordinate are shown in Figure 5.

The parametric equation of blended rolled edge in global coordinate contains four unknowns: x_m , γ_m , a_e , and b_e , which need to be solved further in combination with other conditions.

Since the blended rolled edge and main reflector are expressed by two independent equations, respectively, in order to ensure the continuity between them, it is necessary to guarantee that the n -order curvature radius is continuous in local coordinate at P_j :

$$\left(\frac{\partial^m R_c}{\partial y^m} \right)^{\text{blend}} = \left(\frac{\partial^m R_c}{\partial y^m} \right)^{\text{curve}} \quad m = 1, 2, \dots, n - 1 \tag{23}$$

$$\left(\frac{\partial^n R_c}{\partial y^n} \right)^{\text{blend}} = \left(\frac{\partial^n R_c}{\partial y^n} \right)^{\text{curve}} + y_e \varepsilon_n \tag{24}$$

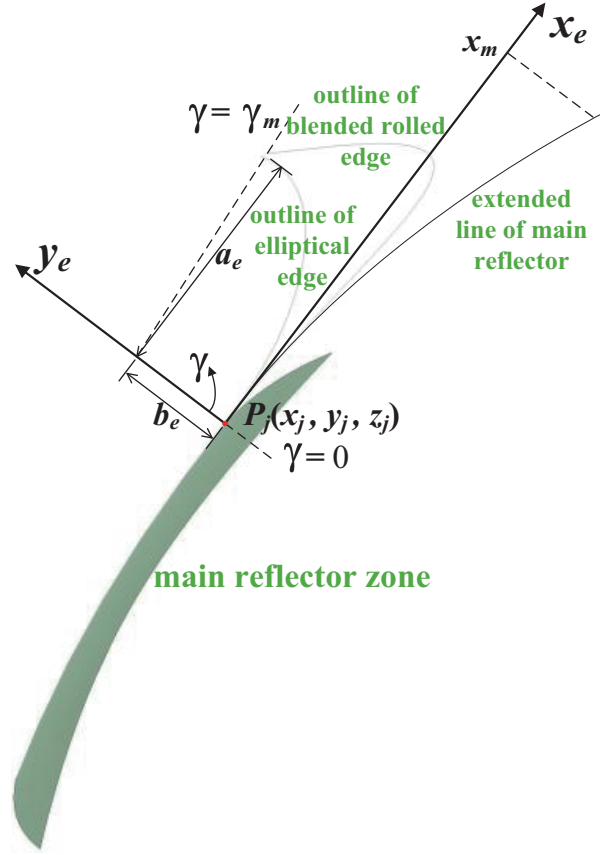


Figure 5. Parameters in local coordinate.

where R_c is the radius of curvature, $n = 4$, which is limited by $b(\gamma)$; y_e represents the residual coefficient; ε_n represents the residual of curvature radius. In order to ensure the continuity, ε_n needs to be as small as possible, and its expression can be written as:

$$\varepsilon_n = \frac{90\pi^4 f_c \left(\sqrt{1 + (y_j/2f_c)^2} \right)^7}{x_m^4} \left(\frac{a_e}{\gamma_m/x_m} + \frac{f_c b_e \left(\sqrt{1 + (y_j/2f_c)^2} \right)^3}{(\gamma_m/x_m)^2} - \frac{1}{2} \right) \quad (25)$$

Assuming that the radian of the rotation angle corresponding to aperture edge is γ_0 , then the curvature radius at this position should not be less than one quarter of the maximum working wavelength [9, 13]:

$$R_c(\gamma_0) \geq \frac{\lambda_{\max}}{4} \quad (26)$$

In order to ensure that the aperture shape is completely consistent with rectangle, it is necessary to fully meet that:

$$\begin{aligned} x'(\gamma_0) &= 0, & y'(\gamma_0) &= 0, \\ x(\gamma_0) &= x_{ax}, & y(\gamma_0) &= y_{ax} \end{aligned} \quad (27)$$

Then the four unknowns can be finally solved through the above three optimization conditions, and the parametric equation of blended rolled edge in global coordinate can be obtained.

3. MODIFIED CONSTRUCTION METHOD OF BLENDED ROLLED EDGE

The traditional construction method of blended rolled edge involves the following three problems:

1) Since the vertical relationship between \hat{y}_e and \hat{p} is not strict, it is impossible to realize the accurate transformation between the local coordinate (x_e, y_e, p) and global coordinate (x, y, z) , which means that the transformation relationship given in Equations (17) and (18) is not tenable, and another local coordinate needs to be selected.

2) Except that the section part of main reflector in the y -axis direction is a parabola, all other sections in local coordinate passing through the center of aperture projection are not, which makes the concept of equivalent parabola inaccurate. Moreover, even if the concept of equivalent parabola is still adopted, the calculation results will be inconsistent due to the arbitrary two groups of points on the equivalent parabola, and the equation of main reflector zone in local coordinate needs to be derived precisely.

3) As the blended rolled edge curves are located in 3D coordinate, in order to ensure that its curvature radius is continuous with that of the main reflector zone, it is necessary to restrict it in global 3D coordinate instead of local coordinate.

The following improvements are made for the above problems, and the other construction steps of blended rolled edge are the same as those in the previous sections.

3.1. Establishing New Local Coordinate Accurately

On the premise of keeping the p -axis unchanged, the intersection line between the plane passing through P_j with normal vector \hat{p} and the tangent plane at P_j is determined as x_e -axis, and there is:

$$\vec{x}_e = \begin{vmatrix} \hat{x} & \hat{y} & \hat{z} \\ x_j & y_j & -2f_c \\ p_1 & p_2 & 0 \end{vmatrix} = 2f_cp_2\hat{x} - 2f_cp_1\hat{y} + (x_jp_2 - y_jp_1)\hat{z} \quad (28)$$

Its unit vector satisfies that:

$$\hat{x}_e = \frac{\vec{x}_e}{|\vec{x}_e|} = x_{p1}\hat{x} + x_{p2}\hat{y} + x_{p3}\hat{z} \quad (29)$$

where,

$$x_{p1} = \frac{2f_cp_2}{\sqrt{(2f_cp_2)^2 + (2f_cp_1)^2 + (x_jp_2 - y_jp_1)^2}} \quad (30)$$

$$x_{p2} = \frac{-2f_cp_1}{\sqrt{(2f_cp_2)^2 + (2f_cp_1)^2 + (x_jp_2 - y_jp_1)^2}} \quad (31)$$

$$x_{p3} = \frac{x_jp_2 - y_jp_1}{\sqrt{(2f_cp_2)^2 + (2f_cp_1)^2 + (x_jp_2 - y_jp_1)^2}} \quad (32)$$

Then the unit vector of y_e -axis satisfies that:

$$\hat{y}_e = \frac{\hat{p} \times \hat{x}_e}{|\hat{p} \times \hat{x}_e|} = y_{p1}\hat{x} + y_{p2}\hat{y} + y_{p3}\hat{z} \quad (33)$$

where,

$$y_{p1} = \frac{x_{p3}p_2}{\sqrt{(x_{p3}p_2)^2 + (x_{p3}p_1)^2 + (x_{p2}p_1 - x_{p1}p_2)^2}} \quad (34)$$

$$y_{p2} = \frac{-x_{p3}p_1}{\sqrt{(x_{p3}p_2)^2 + (x_{p3}p_1)^2 + (x_{p2}p_1 - x_{p1}p_2)^2}} \quad (35)$$

$$y_{p3} = \frac{x_{p2}p_1 - x_{p1}p_2}{\sqrt{(x_{p3}p_2)^2 + (x_{p3}p_1)^2 + (x_{p2}p_1 - x_{p1}p_2)^2}} \quad (36)$$

The position of this local coordinate in global coordinate is shown in black in Figure 4 at P_j .

At this time, the accurate transformation relationship between the local coordinate (x_e, y_e, p) and the global coordinate (x, y, z) at P_j can be expressed as:

$$\begin{bmatrix} x_e \\ y_e \\ p \end{bmatrix} = \begin{bmatrix} x_{p1} & x_{p2} & x_{p3} \\ y_{p1} & y_{p2} & y_{p3} \\ p_1 & p_2 & 0 \end{bmatrix} \begin{bmatrix} x - x_j \\ y - y_j \\ z - z_j \end{bmatrix} \quad (37)$$

$$\begin{bmatrix} x \\ y \\ z \end{bmatrix} = C \begin{bmatrix} x_{p1} & y_{p1} & p_1 \\ x_{p2} & y_{p2} & p_2 \\ x_{p3} & y_{p3} & 0 \end{bmatrix} \begin{bmatrix} x_e \\ y_e \\ p \end{bmatrix} + \begin{bmatrix} x_j \\ y_j \\ z_j \end{bmatrix} \quad (38)$$

where,

$$C = \frac{1}{-x_{p1}y_{p3}p_2 + x_{p2}y_{p3}p_1 + x_{p3}(y_{p1}p_2 - y_{p2}p_1)} \quad (39)$$

3.2. Deriving the Equation of the Main Reflector Zone and Blended Rolled Edge Zone in Local Coordinate Precisely

It is known that the equation of plane passing through P_j with normal vector \hat{p} can be expressed as:

$$p_1(x - x_j) + p_2(y - y_j) = 0 \quad (40)$$

The paraboloid equation of the main reflector zone can be expressed as:

$$x^2 + y^2 = 4f_c z \quad (41)$$

Then the equation of the main reflector zone in local coordinate can be expressed as:

$$\left[1 + \left(\frac{p_2}{p_1}\right)^2\right] y^2 - 2\frac{p_2}{p_1} \left(x_j + \frac{p_2}{p_1} y_j\right) y + \left(x_j + \frac{p_2}{p_1} y_j\right)^2 = 4f_c z \quad (42)$$

Rewrite the equation above with y as the independent variable:

$$x(y) = -\frac{p_2}{p_1} y + \left(x_j + \frac{p_2}{p_1} y_j\right) \quad (43)$$

$$y(y) = y \quad (44)$$

$$z(y) = \left\{ \left[1 + \left(\frac{p_2}{p_1}\right)^2\right] y^2 - 2\frac{p_2}{p_1} \left(x_j + \frac{p_2}{p_1} y_j\right) y + \left(x_j + \frac{p_2}{p_1} y_j\right)^2 \right\} / (4f_c) \quad (45)$$

The expression of the independent variable y in global coordinate can be obtained by solving Equations (21) and (38):

$$y(\gamma) = \frac{C x_m x_{p2}}{\gamma_m} \gamma + y_j \quad (46)$$

Then Equations (43) and (45) can be rewritten as:

$$x(\gamma) = -\frac{C x_m x_{p2} p_2}{p_1 \gamma_m} \gamma + x_j \quad (47)$$

$$z(\gamma) = \frac{p_1^2 + p_2^2}{4f_c} \left(\frac{C x_m x_{p2}}{p_1 \gamma_m}\right)^2 \gamma^2 + \frac{p_1 y_j - p_2 x_j}{2f_c} \frac{C x_m x_{p2}}{p_1 \gamma_m} \gamma + z_j \quad (48)$$

Combined with Equations (22) and (38), the parametric equation of elliptical line with γ as the independent variable in global coordinate can be expressed as:

$$x(\gamma) = C [(a_e \sin \gamma) x_{p1} + b_e (1 - \cos \gamma) y_{p1}] + x_j \quad (49)$$

$$y(\gamma) = C [(a_e \sin \gamma) x_{p2} + b_e (1 - \cos \gamma) y_{p2}] + y_j \quad (50)$$

$$z(\gamma) = C [(a_e \sin \gamma) x_{p3} + b_e (1 - \cos \gamma) y_{p3}] + z_j \quad (51)$$

It can be seen from Eq. (19) that the parametric equation of blended rolled edge with γ as the independent variable in global coordinate can be expressed as:

$$x(\gamma) = \left[-\frac{Cx_mx_{p2}p_2}{p_1\gamma_m}\gamma + x_j \right] [1 - b(\gamma)] + [C((a_e \sin \gamma) x_{p1} + b_e(1 - \cos \gamma) y_{p1}) + x_j] b(\gamma) \quad (52)$$

$$y(\gamma) = \left[\frac{Cx_mx_{p2}}{\gamma_m}\gamma + y_j \right] [1 - b(\gamma)] + [C((a_e \sin \gamma) x_{p2} + b_e(1 - \cos \gamma) y_{p2}) + y_j] b(\gamma) \quad (53)$$

$$z(\gamma) = \left[\frac{p_1^2 + p_2^2}{4f_c} \left(\frac{Cx_mx_{p2}}{p_1\gamma_m} \right)^2 \gamma^2 + \frac{p_1 y_j - p_2 x_j}{2f_c} \frac{Cx_mx_{p2}}{p_1\gamma_m} \gamma + z_j \right] [1 - b(\gamma)] + [C((a_e \sin \gamma) x_{p3} + b_e(1 - \cos \gamma) y_{p3}) + z_j] b(\gamma) \quad (54)$$

3.3. Optimizing the Continuity Condition of Curvature Radius

The continuity condition of curvature radius needs to be extended from one dimension to two dimensions, which means that the n -order curvature radius of blended rolled edge curve and the section of main reflector need to be continuous in the y direction and z direction at P_j simultaneously

$$\left(\frac{\partial^m R_c}{\partial y^m} \right)^{\text{blend}} = \left(\frac{\partial^m R_c}{\partial y^m} \right)^{\text{curve}} \quad m = 1, 2, \dots, n - 1 \quad (55)$$

$$\left(\frac{\partial^n R_c}{\partial y^n} \right)^{\text{blend}} = \left(\frac{\partial^n R_c}{\partial y^n} \right)^{\text{curve}} + y_\varepsilon \varepsilon_n \quad (56)$$

$$\left(\frac{\partial^m R_c}{\partial z^m} \right)^{\text{blend}} = \left(\frac{\partial^m R_c}{\partial z^m} \right)^{\text{curve}} \quad m = 1, 2, \dots, n - 1 \quad (57)$$

$$\left(\frac{\partial^n R_c}{\partial z^n} \right)^{\text{blend}} = \left(\frac{\partial^n R_c}{\partial z^n} \right)^{\text{curve}} + z_\varepsilon \varepsilon_n \quad (58)$$

where R_c represents the curvature radius; n decreases to 3 due to the increasing dimension; y_ε represents the residual coefficient in y direction; z_ε represents the residual coefficient in z direction; ε_n represents the residual of curvature radius. In order to ensure the continuity, ε_n needs to be as small as possible, which can be written as:

$$\varepsilon_n = \frac{[y'(y'z'''' - y''''z') - x'(x''''z' - x'z''''')] [(x')^2 + (y')^2 + (z')^2]^{3/2}}{(z'')^4 [(y')^2 + (x')^2]^{5/2}} \quad (59)$$

where x' , y' , z' , z'' , x'''' , y'''' and z'''' represent the first derivative, second derivative, and fifth derivative of x , y , z components of blended rolled edge curve equation, respectively.

4. COMPARISON BETWEEN TRADITIONAL METHOD AND MODIFIED METHOD

It is known that the parameters of blended rolled edge are that [9, 13] the observation frequency is 2 GHz; the focal length is 7.25'; the absolute length of edge is 3.5'; the maximum and minimum values of aperture in the x -axis direction are 7.5' and -7.5'; the maximum and minimum values in the y -axis direction are 15' and 2'; and the distance between observation point and aperture in the z -axis direction is 20'.

According to [9, 13] and the modified construction method in this paper, the outline and aperture of blended rolled edge reflector are shown in Figure 6, Figure 7, and Figure 8, respectively. The outline part (a) only gives the projection of right blended rolled edge curves on rectangular aperture, and the left side can be obtained symmetrically through the right side.

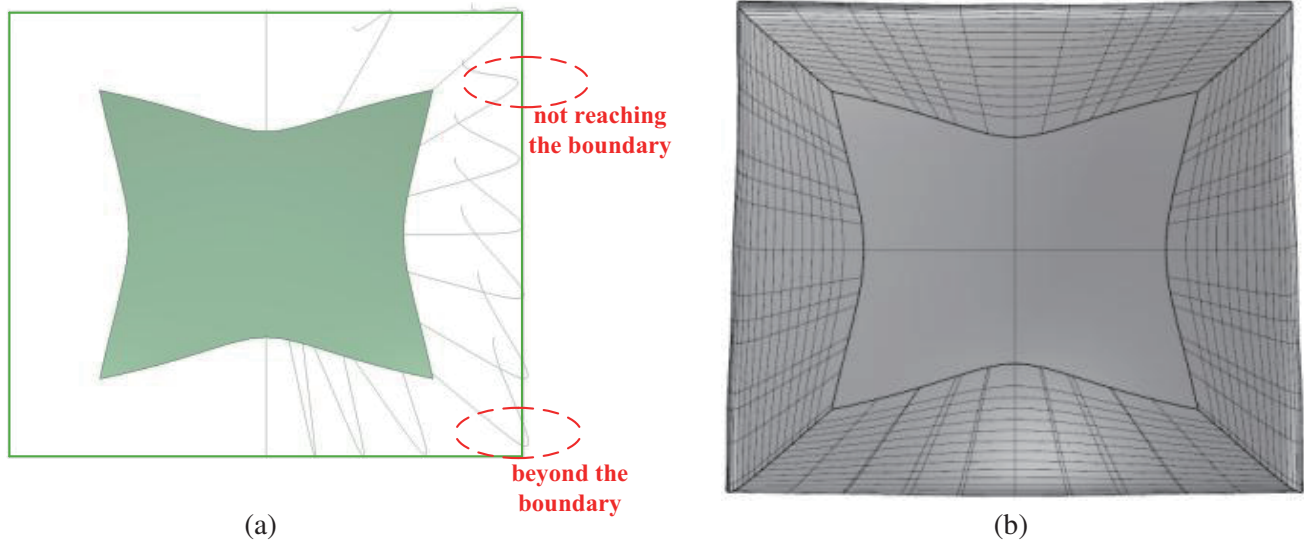


Figure 6. Model in Reference [9]. (a) Outline of blended rolled edge. (b) Aperture of blended rolled edge reflector.

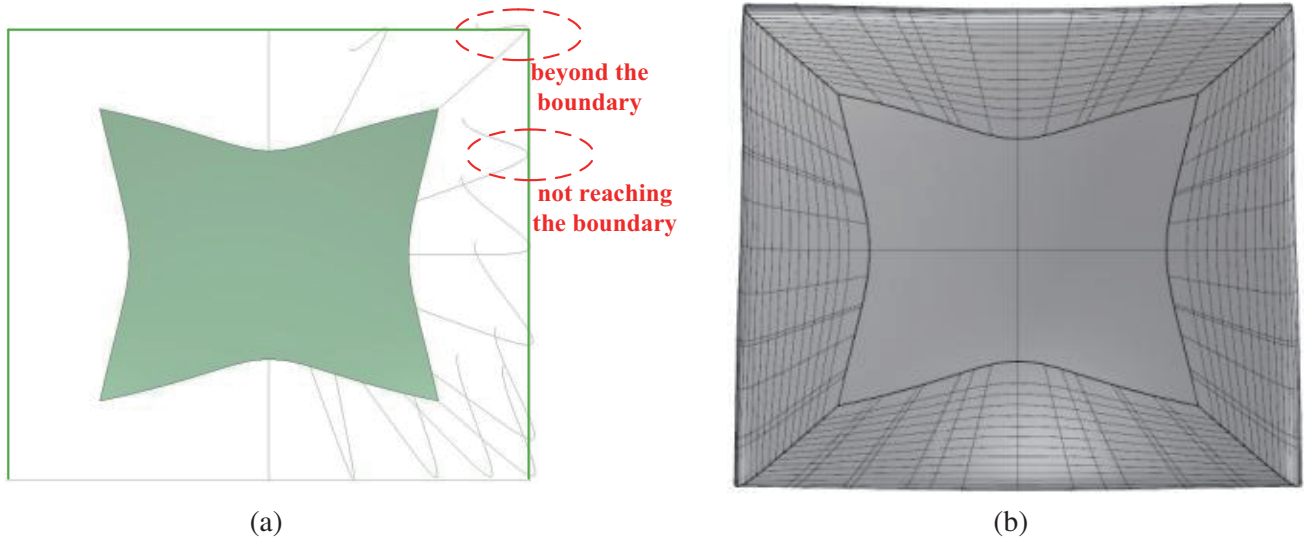


Figure 7. model in Reference [13]. (a) Outline of blended rolled edge. (b) Aperture of blended rolled edge reflector.

It can be seen from the above results that in terms of geometric construction, the shape of blended rolled edge reflector obtained by traditional construction method deviates greatly from the rectangular aperture, while that obtained by modified construction method is completely consistent with the rectangular aperture.

The electrical performance of the reflectors above is simulated and analyzed below. Before that, the following adjustments need to be made:

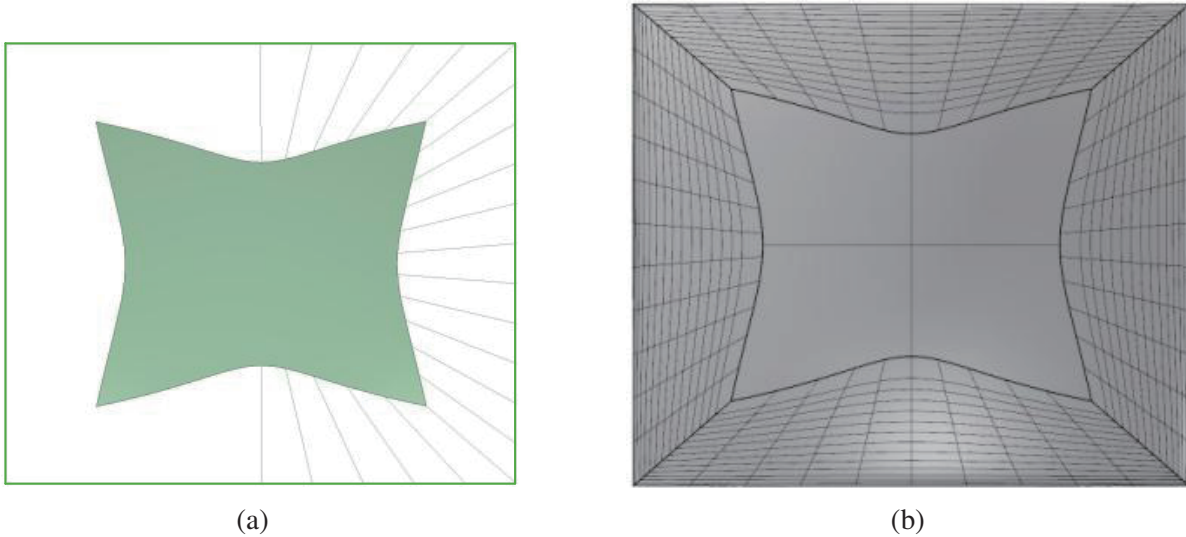
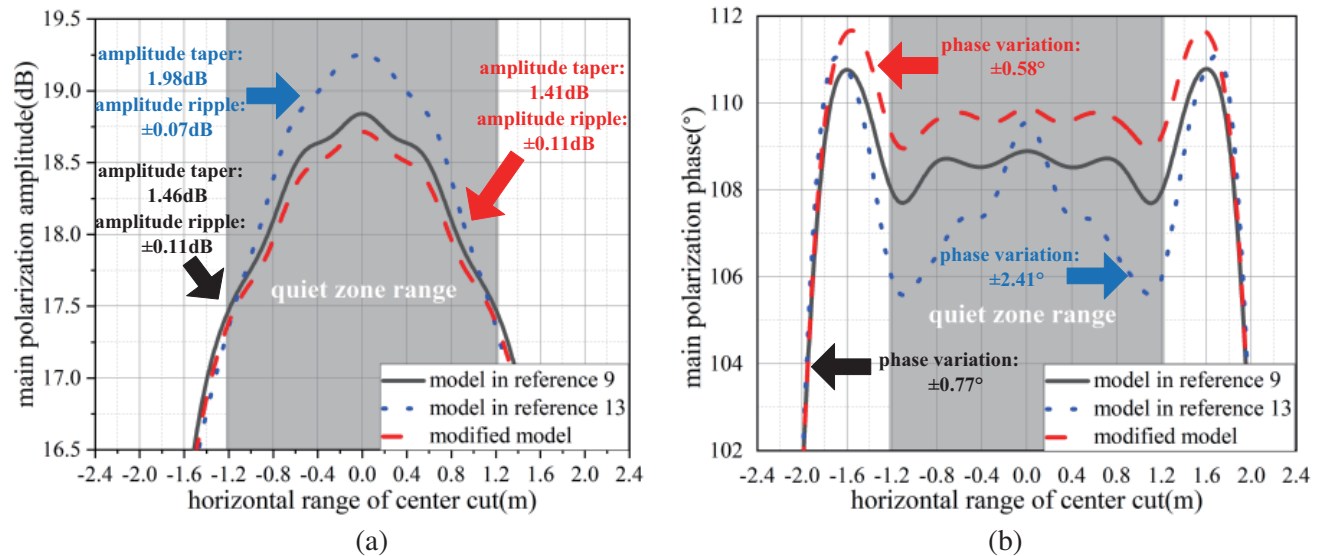


Figure 8. Modified model. (a) Outline of blended rolled edge. (b) Aperture of blended rolled edge reflector.

- 1) Adjusting the observation frequency. The advantage of blended rolled edge reflector lies in the low-frequency performance, and the edge length is usually $3 \sim 5\lambda_{\max}$ [21]. As the current absolute length of the edge is $3.5'$, the observation frequency should be chosen as 0.85 GHz corresponding to $3\lambda_{\max}$, or 1.4 GHz corresponding to $5\lambda_{\max}$;
- 2) Adjusting the observation position. Generally speaking, the distance between reflector vertex and quiet zone center is $5/3f_c$ [21]. Therefore, the distance between the observation point and reflector vertex in the z -axis direction is set to $12.08'$.

The Gaussian beam with 1 dB beam width of 47° is used as the feed to irradiate these reflectors, and its elevation angle is set to 87° . The amplitude and phase curves of quiet zone are shown in Figure 9 and Figure 10, which are simulated at the observation position by using the method of moments (MoM).

It can be seen from the above results that in terms of electrical performance, compared with the reflector obtained by traditional construction method, the main polarization amplitude and phase of the reflector obtained by modified construction method are much better, especially the amplitude of vertical center cuts. Compared with the results in [9] and [13], the overall amplitude flatness of vertical



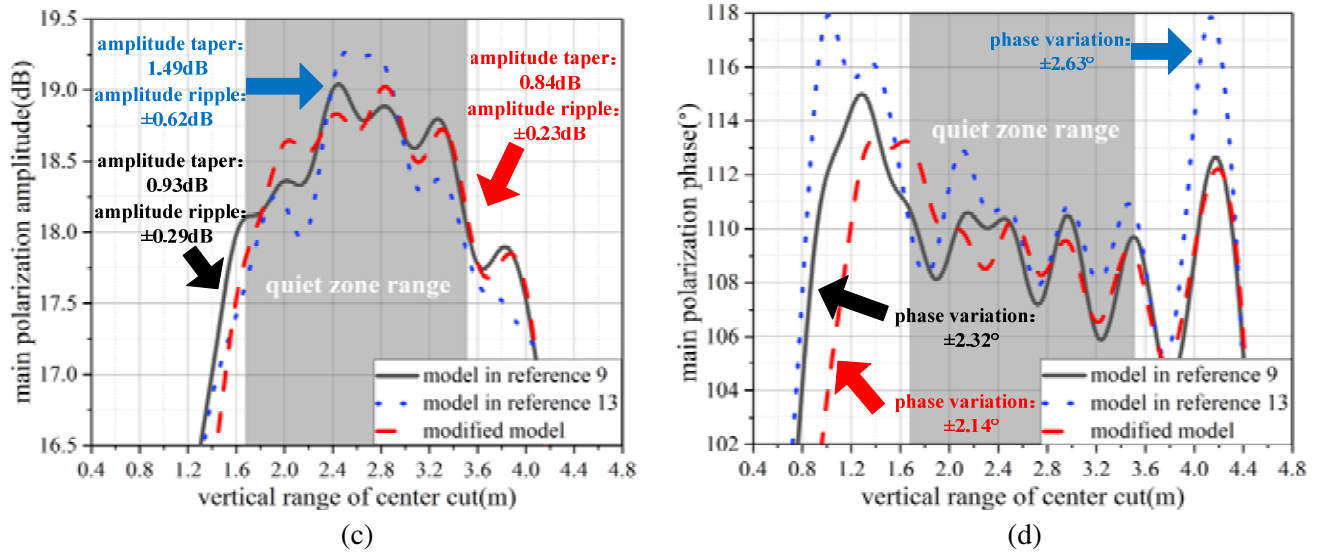
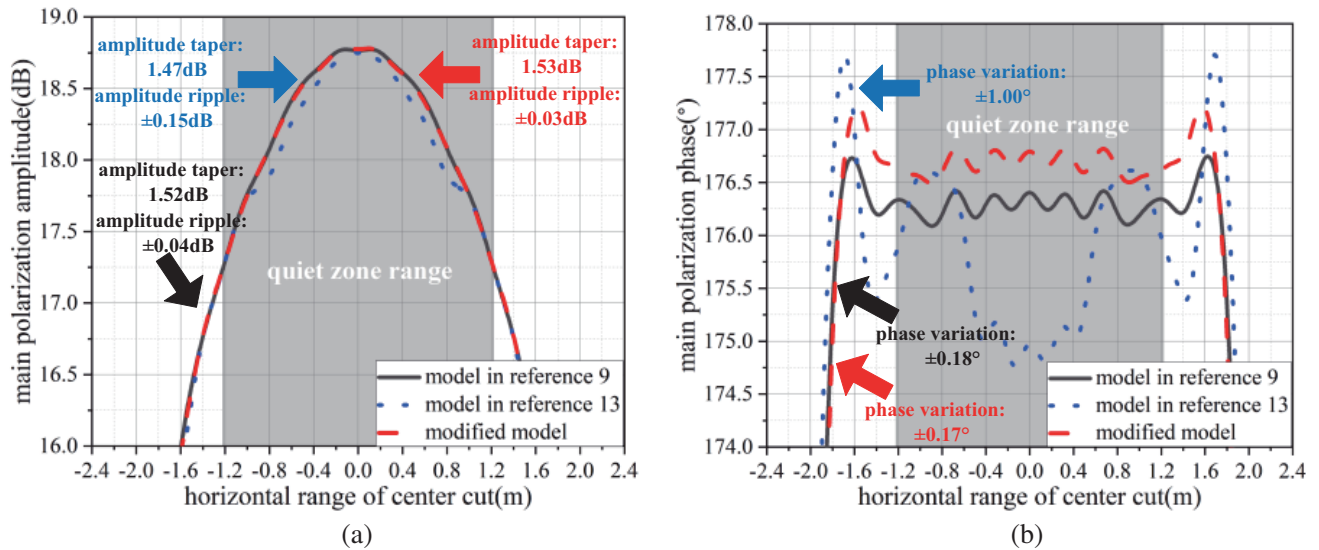


Figure 9. Comparison on main polarization amplitude and phase of center cuts at 0.85 GHz. (a) Distribution of main polarization amplitude of horizontal center cut. (b) Distribution of main polarization phase of horizontal center cut. (c) Distribution of main polarization amplitude of vertical center cut. (d) Distribution of main polarization phase of vertical center cut.

center cuts of the modified one at 0.85 GHz is improved by about 0.21 dB and 1.33 dB, respectively, while that at 1.4 GHz is improved by about 0.25 dB and 0.68 dB, respectively. In addition, the reflector obtained by modified construction method has good step drop characteristics at the lower end of quiet zone, which reduces the design difficulty of the chamber environment. Compared with the reference results, the step drop amplitudes at 0.85 GHz and 1.4 GHz are about 1 dB and 0.8 dB, respectively. Due to the proper treatment of aperture edge and connection relationship between the main reflector zone and blended rolled edge zone geometrically, there is no doubt that good electrical performance can be obtained.



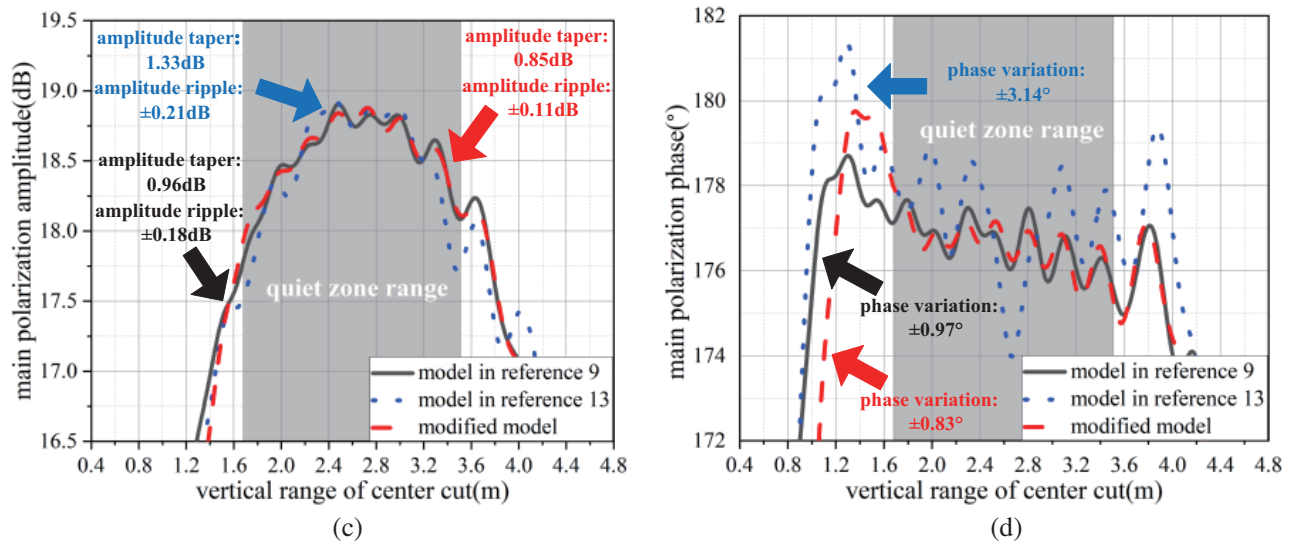


Figure 10. Comparison on main polarization amplitude and phase of center cuts at 1.4 GHz. (a) Distribution of main polarization amplitude of horizontal center cut. (b) Distribution of main polarization phase of horizontal center cut. (c) Distribution of main polarization amplitude of vertical center cut. (d) Distribution of main polarization phase of vertical center cut.

5. DESIGN OF BLENDED ROLLED EDGE REFLECTOR

In order to further illustrate the correctness of modified construction method proposed in this paper, a blended rolled edge reflector with minimum working frequency of 0.8 GHz and quiet zone size of 2 m is designed. The absolute length of the blended rolled edge is determined as $5\lambda_{\max}$, i.e., 1.875 m, and the utilization rate of the reflector is set to 40%, then the maximum and minimum values of aperture in the x -axis direction are 2.5 m and -2.5 m, respectively, and the maximum and minimum values in the y -axis direction are 5.1 m and 0.1 m, respectively. In order to ensure that the cross polarization amplitude is less than -28 dB, the focal diameter ratio is determined as 0.9, then the focal length is 6.36 m. The center of quiet zone is located at $5/3f_c$ from reflector vertex in z -axis direction, i.e., 10.6 m. The aperture projection of this designed reflector is shown in Figure 11.

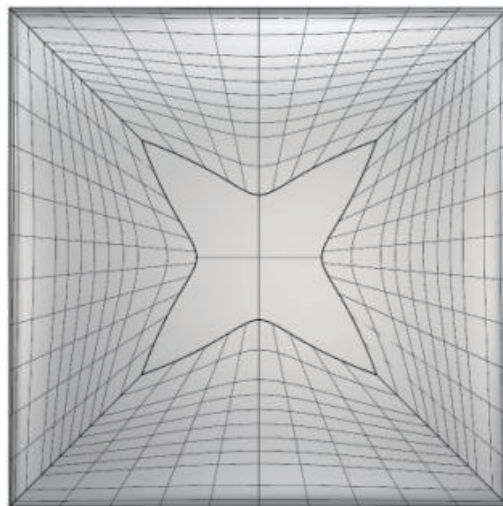


Figure 11. Aperture projection of the designed reflector.

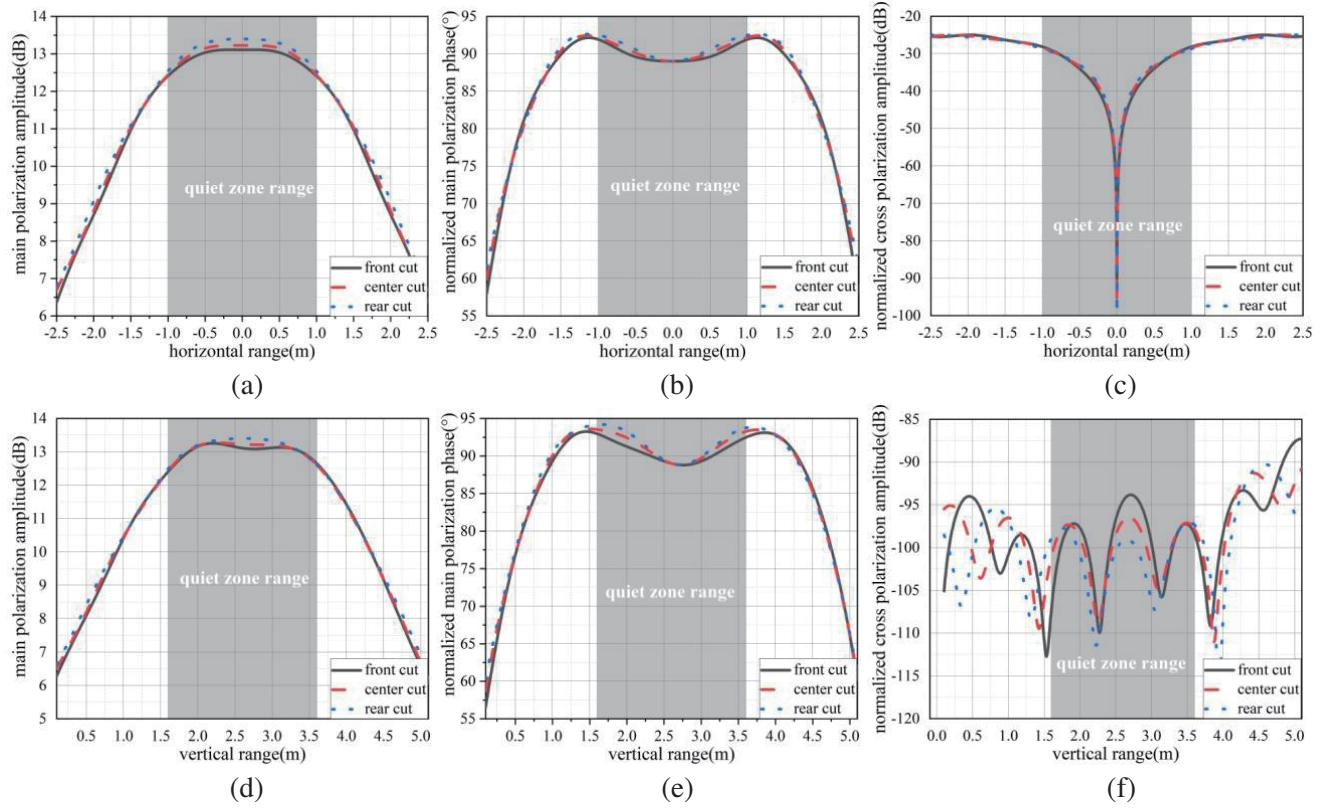
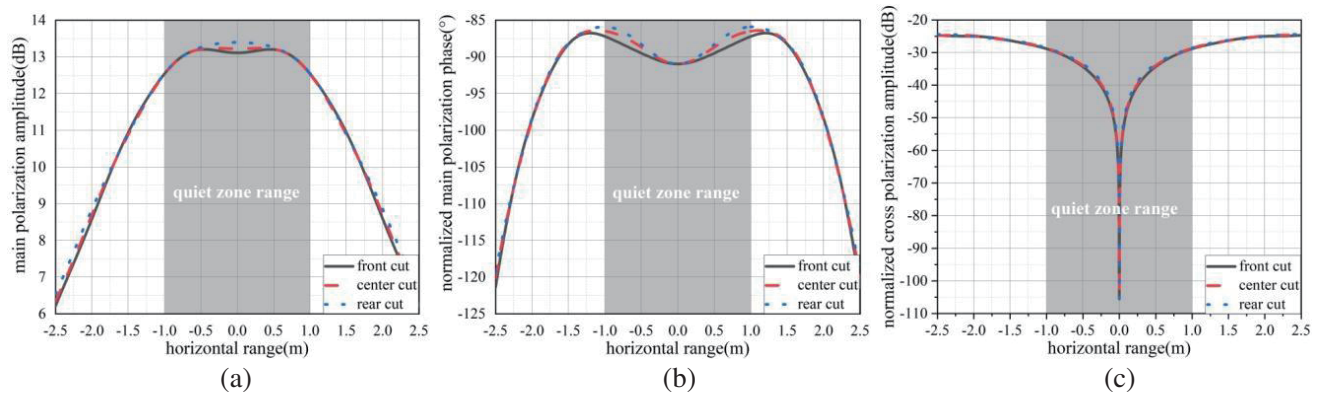


Figure 12. Results of amplitude and phase in quiet zone under horizontal polarization. (a) Distribution of main polarization amplitude of horizontal cuts. (b) Distribution of main polarization phase of horizontal cuts. (c) Distribution of cross polarization amplitude of horizontal cuts. (d) Distribution of main polarization amplitude of vertical cuts. (e) Distribution of main polarization phase of vertical cuts. (f) Distribution of cross polarization amplitude of vertical cuts.

The Gaussian beam with 1 dB beam width of 27° is used as the feed to irradiate the reflector, and its elevation angle is set to 26° . The MoM is used to simulate the amplitude and phase of front cuts, center cuts, and rear cuts at 0.8 GHz. The simulation results under two feed polarization states are shown in Figure 12 and Figure 13, respectively.

It can be seen from the above results that the maximum value of amplitude taper is 0.82 dB; the maximum value of amplitude ripple is ± 0.26 dB; the maximum value of cross polarization amplitude is -28.2 dB; and the maximum value of phase variation is $\pm 3.2^\circ$, which is much better than the requirements of conventional design indexes in quiet zone.



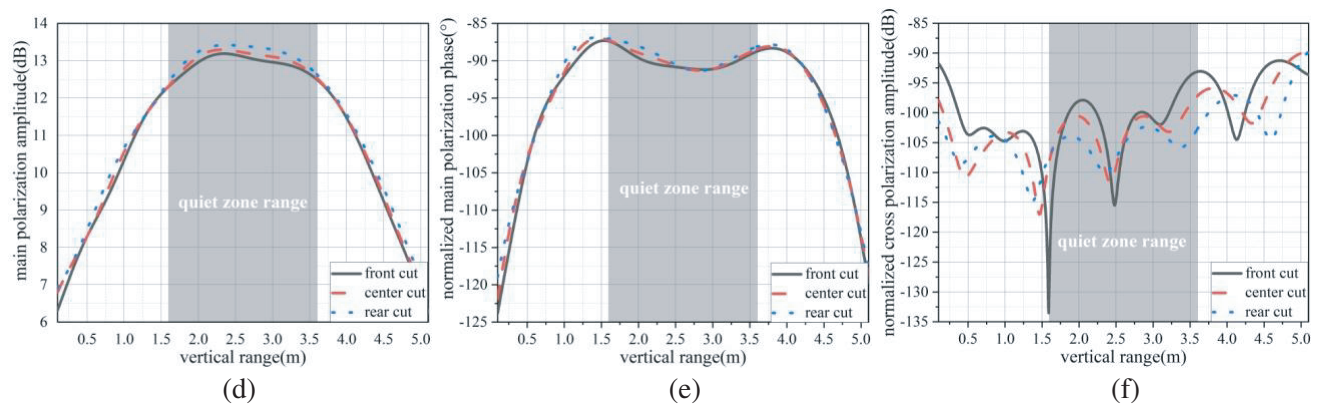


Figure 13. Results of amplitude and phase in quiet zone under vertical polarization. (a) Distribution of main polarization amplitude of horizontal cuts. (b) Distribution of main polarization phase of horizontal cuts. (c) Distribution of cross polarization amplitude of horizontal cuts. (d) Distribution of main polarization amplitude of vertical cuts. (e) Distribution of main polarization phase of vertical cuts. (f) Distribution of cross polarization amplitude of vertical cuts.

6. CONCLUSION

In order to obtain the blended rolled edge reflector whose aperture size and electromagnetic performance fully meet the design requirements, this paper improves the traditional construction method of blended rolled edge from three aspects: accurately establishing new local coordinate, precisely deriving the equation of main reflector zone and blended rolled edge zone in local coordinate, and optimizing the continuity condition of curvature radius. On this basis, a blended rolled edge reflector with minimum working frequency of 0.8 GHz and quiet zone size of 2 m is designed. The simulation results show that the performance of the blended rolled edge reflector constructed by proposed method is better than that obtained by the traditional construction method, and the designed reflector has excellent performance, which can be used in practical engineering. The work in this paper provides theoretical support for the accurate model construction, efficient performance optimization, and wide engineering application of blended rolled edge reflector.

REFERENCES

1. Johnson, R. C., H. A. Ecker, and R. A. Moore, "Compact range techniques and measurements," *IEEE Transactions on Antenna and Propagation*, Vol. 17, No. 5, 569–576, 1969.
2. Jiang, Y.-Q., C.-J. Mo, W.-Q. Chen, et al., "Research on serrations of reflector used in CATR," *2019 Photonics & Electromagnetics Research Symposium*, 1665–1669, Xiamen, China, 2019.
3. Burnside, W. D., M. C. Gilreath, and B. M. Kent, "Rolled edge modification of compact range reflector," *Antenna Measurement Techniques Association Symposium*, 4B3-1–4B3-28, San Diego, America, 1984.
4. Burnside, W. D., A. K. Dominek, and R. Barger, "Blended surface concept for a compact range reflector," *Antenna Measurement Techniques Association Symposium*, 10-1–10-10, Melbourne, Australia, 1985.
5. Pistorius, C. W. I. and W. D. Burnside, "A concave edged reflector with blended rolled surface terminations for compact range applications," *Antenna Measurement Techniques Association Symposium*, 123–128, Ottawa, Canada, 1986.
6. Pistorius, C. W. I., "New main reflector, subreflector and dual chamber concepts for compact range applications," Ph.D. dissertation, The Ohio State University, 1986.

7. Pistorius, C. W. I. and W. D. Burnside, "The design of blended rolled edges for compact range main reflectors," *The 5th International Conference on Antennas and Propagation*, 1874–1879, England, Britain, 1987.
8. Burnside, W. D., M. C. Gilreath, B. M. Kent, et al., "Curved edge modification of compact range reflector," *IEEE Transactions on Antenna and Propagation*, Vol. 35, No. 2, 176–182, 1987.
9. Pistorius, C. W. I. and W. D. Burnside, "An improved main reflector design for compact range applications," *IEEE Transactions on Antenna and Propagation*, Vol. 35, No. 3, 342–347, 1987.
10. Gupta, I. J. and W. D. Burnside, "A physical optics correction for backscattering from curved surfaces," *IEEE Transactions on Antenna and Propagation*, Vol. 35, No. 5, 553–561, 1987.
11. Pistorius, C. W. I., G. C. Clerici, and W. D. Burnside, "A dual chamber Gregorian subreflector system for compact range applications," *IEEE Transactions on Antenna and Propagation*, Vol. 37, No. 3, 305–313, 1989.
12. Ellingson, S. W., I. J. Gupta, and W. D. Burnside, "Analysis of blended rolled edge reflectors using numerical UTD," *IEEE Transactions on Antenna and Propagation*, Vol. 38, No. 12, 1969–1971, 1990.
13. Gupta, I. J., K. P. Ericksen, and W. D. Burnside, "A method to design blended rolled edges for compact range reflectors," *IEEE Transactions on Antenna and Propagation*, Vol. 38, No. 6, 853–861, 1990.
14. Gupta, I. J. and W. D. Burnside, "Compact range measurement systems for electrically small test zones," *IEEE Transactions on Antenna and Propagation*, Vol. 39, No. 5, 632–638, 1991.
15. Lee, T.-H. and W. D. Burnside, "Performance trade-off between serrated edge and blended rolled edge compact range reflectors," *IEEE Transactions on Antenna and Propagation*, Vol. 44, No. 1, 87–96, 1996.
16. Lee, T.-H. and W. D. Burnside, "Compact range reflector edge treatment impact on antenna and scattering measurements," *IEEE Transactions on Antenna and Propagation*, Vol. 45, No. 1, 57–65, 1997.
17. Proctor, J. R., D. R. Smith, et al., "Compact range rolled edge reflector design, fabrication, installation and mechanical qualification," *Antenna Measurement Techniques Association Symposium*, 285–292, Georgia, America, 2004.
18. Muñoz-Acevedo, A., S. Burgos, and M. Sierra-Castañer. "Performance comparison between serrated edge and rolled edge reflectors inside CATR facilities," *European Conference on Antennas and Propagation*, 3586–3590, IEEE Press, Rome, Italy, 2011.
19. Tellakula, A., W. R. Griffin, and S. T. McBride, "Predicting the performance of a very large, wideband rolled-edge reflector," *Antenna Measurement Techniques Association Symposium*, 386–392, Suwanee, America, 2015.
20. Tellakula, A., W. R. Griffin, and S. T. McBride, "Quiet zone qualification of a very large, wideband rolled-edge reflector," *Antenna Measurement Techniques Association Symposium*, 245–251, Georgia, America, 2016.
21. David, J. W., M. John, and T. M. Scott, "Advancements in achieving what is asked of a compact range," *Antenna Measurement Techniques Association Symposium*, 574–580, Columbus, America, 2013.